

Using boundary methods to compute the Casimir energy

F.C. Lombardo¹, F.D. Mazzitelli¹, and P.I. Villar^{1,2}

¹ *Departamento de Física Juan José Giambiagi, FCEyN UBA, Facultad de Ciencias Exactas y Naturales, Ciudad Universitaria, Pabellón I, 1428 Buenos Aires, Argentina*

² *Computer Applications on Science and Engineering Department, Barcelona Supercomputing Center (BSC), 29, Jordi Girona 08034 Barcelona, Spain*

We discuss new approaches to compute numerically the Casimir interaction energy for waveguides of arbitrary section, based on the boundary methods traditionally used to compute eigenvalues of the 2D Helmholtz equation. These methods are combined with the Cauchy's theorem in order to perform the sum over modes. As an illustration, we describe a point-matching technique to compute the vacuum energy for waveguides containing media with different permittivities. We present explicit numerical evaluations for perfect conducting surfaces in the case of concentric corrugated cylinders and a circular cylinder inside an elliptic one.

Keywords: Style file; L^AT_EX; Proceedings; World Scientific Publishing.

1. Introduction

In this paper we will be concerned with the numerical calculation of the Casimir interaction energy in geometries with translational invariance along one direction, i.e. very long cylinders of arbitrary section. For the sake of simplicity, we will first discuss the case of a massless quantum scalar field that satisfies Dirichlet or Neumann boundary conditions on the surfaces of the cylinders. As we will see, in some particular situations the generalization to the electromagnetic field and/or more general boundary conditions will be straightforward.

The Casimir energy is formally given by

$$E_{12}(\sigma) = \lim_{\sigma \rightarrow 0} \frac{1}{2} \sum_p (e^{-\sigma w_p} w_p - e^{-\sigma \tilde{w}_p} \tilde{w}_p), \quad (1)$$

where w_p are the eigenfrequencies of the scalar field satisfying the appropriate boundary conditions on the surfaces of the shells, and \tilde{w}_p are those corresponding to a situation in which the distances between the shells is

very large. The subindex p denotes the set of quantum numbers associated to each eigenfrequency. We have introduced an exponential cutoff for high frequency modes.

For the particular geometry considered here, $p = (n, k_z)$ and the eigenfrequencies are of the form $\omega_{n,k_z} = \sqrt{k^2 + \lambda_n^2}$, where k_z is a continuous variable associated to the translational invariance along the z-direction and λ^2 are the eigenvalues of the Laplacian on the two-dimensional transversal section Σ contained in the plane (x,y):

$$\Delta^2 u = -\lambda^2 u . \quad (2)$$

The eigenfunctions $u(\mathbf{x})$ satisfy Dirichlet or Neumann boundary conditions on Γ , the boundary of Σ .

The Helmholtz equation (2) arises in many branches of physics, from the vibration of membranes to quantum billiards, and there are a plethora of methods to compute numerically its eigenfunctions and eigenvalues.¹ Among them, the "boundary methods" are based on the following strategy: the solution u is written as a (finite) linear combination of basis functions that satisfy Helmholtz equation inside Σ . The coefficients of the linear combination are chosen in such a way that the boundary conditions are satisfied at a finite number of points on Γ . The linear system of equations that determine the coefficients has a non trivial solution only for some particular values of λ , the eigenvalues of the system.

For example, in the Point Matching Method (PMM),² one expands the eigenfunction u in terms of a basis of solutions of the Helmholtz equation in free space $\varphi_j^{(\lambda)}(\mathbf{x})$

$$u(\mathbf{x}) = \sum_{j=1}^{\infty} a_j \varphi_j^{(\lambda)}(\mathbf{x}) . \quad (3)$$

In the numerical calculation this expansion is truncated at given $j = N$, and the boundary conditions are imposed on N points on Γ . These boundary conditions become a set of homogeneous, linear equations for the unknown coefficients a_j ($Ma = 0$, with M a λ -dependent $N \times N$ matrix) which has nontrivial solutions only when $\det M = 0$. The last equation can be used to determine numerically the eigenvalues λ_n .

In a similar approach, known as the Method of Fundamental Solutions (MFS),³ the eigenfunction u is expanded in terms of solutions of the Helmholtz equation with a point source at an arbitrary location \mathbf{s}_j , that we

denote by $u_\lambda(\mathbf{x}, \mathbf{s}_j)$

$$u(\mathbf{x}) = \sum_{j=1}^{\infty} b_j u_\lambda(\mathbf{x}, \mathbf{s}_j). \quad (4)$$

If the sources are located *outside* Σ , this is a solution of the homogeneous Helmholtz equation *inside* Σ . Once again, the sum is truncated at $j = N$, and the coefficients b_j are determined by solving the linear system that results when imposing the boundary conditions on a finite number of points on Γ . The roots of the determinant of the associated matrix are the eigenfrequencies of the problem. This is the simplest version of the MFS, in which the locations of the sources are fixed.

One can find in the literature discussions about spurious solutions, improvements and alternative methods to find the eigenvalues. We refer the reader to Refs.^{1,4} for more details.

A crucial point is that, at a practical level, the knowledge of the spectrum of the Helmholtz equation is not enough to compute the Casimir energy. The reason is that the numerical evaluation of the sum over modes in Eq.(1) is extremely unstable,⁵ and one has to subtract very large numbers to compute the finite interaction energy. The calculation is complicated even for the simplest case of Casimir effect in $1 + 1$ dimensions.

Instead of performing explicitly the summation, it is far more efficient to combine the methods mentioned previously with the Cauchy's theorem

$$\frac{1}{2\pi i} \int_C dz \, z e^{-\sigma z} \frac{d}{dz} \ln f(z) = \sum_i z_i e^{-\sigma z_i}, \quad (5)$$

where $f(z)$ is an analytic function in the complex z plane within the closed contour C , with simple zeros at z_1, z_2, \dots within C . We use this result to replace the sum over the eigenvalues of the Helmholtz equation in the Casimir energy Eq.(1) by a contour integral. In this way, it is not necessary to solve numerically the equation $\det M = 0$ for the eigenvalues, but to take $f = \det M$ in the Cauchy's theorem. In other words, if in the numerical method to solve the Helmholtz equation the eigenvalues are the roots of a given function, one can integrate this function in the complex plane in order to get the Casimir energy. The combination of the use of numerical methods to compute the eigenvalues with the Cauchy's theorem is the main idea we want to put forward in this paper.

In the next Section we will describe the simplest version of the PMM to a situation in which the surfaces separate regions of different permittivities, generalizing our previous results⁶ for perfect conductors. In Sections 3 and 4

we will review some numerical evaluations of the Casimir interaction energy for perfect conductors. In Section 5 we include our final remarks.

2. Point-Matching Numerical Approach

A media-separated waveguide presents an interesting setup for the application of the PMM. This technique has been widely used to solve eigenvalue problems in many areas of engineering science.² The boundary conditions are imposed at a finite number of points around the periphery of both media.

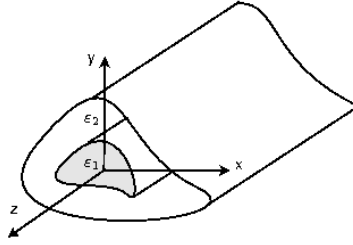


Fig. 1. A two-separated media waveguide in which one conductor encloses two different dielectric media. Each has arbitrary cross section.

For the sake of concreteness, we will bear in mind the situation in which one perfect conductor encloses two dielectric media, as shown in Fig.1, although the method could be applied to more general cases.

The general solution of the Helmholtz equation in region I (inside the inner cylinder) is

$$u = \sum_m A_m J_m(\lambda^{(I)} r) e^{im\theta}, \quad (6)$$

while in region II (annular region)

$$u = \sum_m [B_m J_m(\lambda^{(II)} r) + C_m H_m^{(1)}(\lambda^{(II)} r)] e^{im\theta}, \quad (7)$$

where (r, θ) are polar coordinates, and J_m and $H_m^{(1)}$ are the m -th order Bessel functions. The constants A_m, B_m and C_m are determined by the boundary conditions. In both equations we have defined $\lambda^{(a)} = \sqrt{\epsilon_a \omega^2 - k_z^2}$.

We assume the outer surface to be a "perfect conductor", and impose Dirichlet boundary conditions on a finite number of points (r_q, θ_q) of C_2 :

$$0 = \sum_{m=-S}^S [B_m J_m(\lambda^{(II)} r_q) + C_m H_m^{(1)}(\lambda^{(II)} r_q)] e^{im\theta_q}, \quad (8)$$

(alternatively, for the TE modes of the electromagnetic field, one should impose Neumann boundary conditions). The surface C_1 as a dielectric interphase separating media ϵ_1 and ϵ_2 , and therefore we impose continuity of the field and its derivative:

$$\begin{aligned} \sum_{m=-S}^S A_m J_m(\lambda^{(I)} r_p) e^{im\theta_p} &= \sum_{m=-S}^S [B_m J_m(\lambda^{(II)} r_p) + C_m H_m^{(1)}(\lambda^{(II)} r_p)] e^{im\theta_p} \\ \sum_{m=-S}^S A_m J'_m(\lambda^{(I)} r_p) e^{im\theta_p} &= \frac{\lambda^{(II)}}{\lambda^{(I)}} \sum_{m=-S}^S [B_m J'_m(\lambda^{(II)} r_p) + C_m H'_m^{(1)}(\lambda^{(II)} r_p)] e^{im\theta_p}, \end{aligned} \quad (9)$$

where (r_p, θ_p) are points on the curve C_1 .

The boundary conditions can be written, in matrix form, as

$$\begin{aligned} 0 &= N_1 B + N_2 C, \\ R_1 A &= M_1 B + M_2 C, \\ R_2 A &= M'_1 B + M'_2 C. \end{aligned} \quad (10)$$

Eliminating the coefficients A_m we end with

$$N_1 B + N_2 C = 0, \quad P_1 B + P_2 C = 0, \quad (11)$$

where P_1 and P_2 can be written as

$$P_1 = M_1 - R_1 R_2^{-1} M'_1, \quad P_2 = M_2 - R_1 R_2^{-1} M'_2. \quad (12)$$

It is worthy to note that as $R_1 R_2^{-1}$ is proportional to λ_2/λ_1 , then $R_1 R_2^{-1} \rightarrow 0$ when $\epsilon_1 \rightarrow \infty$. Thus, the matrices $P_1 \rightarrow M_1$ and $P_2 \rightarrow M_2$, re-obtaining in this way, the usual perfect conductor wave-guide case studied in.⁶

For the system of Eq.(11) to have non trivial solutions, the determinant must be zero, i.e.

$$\det \begin{bmatrix} N_1 & N_2 \\ P_1 & P_2 \end{bmatrix} = \det P_2 \cdot \det N_1 \cdot \det(1 - N_2 P_2^{-1} P_1 N_1^{-1}) = 0. \quad (13)$$

This equation determines the eigenfrequencies associated to the geometry. However, as already mentioned, in order to compute the Casimir energy it is not necessary to find each eigenvalue but to integrate the determinant $Q = \det(1 - N_2 P_2^{-1} P_1 N_1^{-1})$ in the complex plane.

We have developed a numerical Fortran routine in order to evaluate the Casimir interaction energy in the case in which the field satisfies Dirichlet or Neumann boundary conditions on both curves C_1 and C_2 . In this case one should consider the fields only in region II with $\epsilon_2 = 1$. After some straightforward steps one can re-write the Casimir energy as a single integral in the imaginary axis $iy = \lambda^{(II)}$. For Dirichlet boundary conditions the result is

$$E_{12} = \frac{L}{4\pi} \int_0^\infty dy \, y \ln Q(iy), \quad (14)$$

while for Neumann boundary conditions one can derive a similar expression with a different function Q . It is worth to stress that these Casimir energies correspond to those of TM and TE modes of the electromagnetic field in the presence of perfect conductors.

3. Cylindrical rack and pinion

When two concentric cylinders have corrugations, the vacuum energy produces a torque that could, in principle, make one cylinder rotate with respect to the other. This “cylindrical rack and pinion” has been proposed in Ref.,⁷ where the torque has been computed using the proximity force approximation. It was further analyzed in,⁸ where the authors obtained perturbative results for Dirichlet boundary conditions in the limit of small amplitude corrugations. In this Section, we numerically evaluate the Casimir interaction energy for two concentric corrugated, perfect conductor cylinders. The cylinders have radii a and b , and we will denote by $r_- = b - a$ the mean distance between them and by $r_+ = a + b$ the sum of the radii. We will use the notation $\alpha = b/a$. The points in the mesh, that give us the corrugated cylinder boundaries, are described by the following functions:

$$h_a(\theta) = h \sin(\nu\theta) \quad ; \quad h_b(\theta) = h \sin(\nu\theta + \phi_0), \quad (15)$$

where h is the corrugation amplitude and ν is the frequency associated with these corrugations. The Casimir torque can be calculated by taking the derivative of the interaction energy with respect to the shifted angle $\mathcal{T} = -\partial E_{12}/\partial \phi_0$.

In Fig.2 we show the numerical evaluation of the TM Casimir interaction energy for this geometry. The plot shows the results obtained using the PMM with $\alpha = 2$ and corrugation frequency $\nu = 3$, for different values of the amplitude of the corrugation h . As expected the amplitude of the oscillations grows with h . For each value of h we have performed a numerical

fit of the data in order to compare with the analytical prediction. With dotted lines we have plotted the fit $y(x) = A * \cos(x)$ for each curve in Fig.2. The agreement between dots and dotted lines is extremely good. Similar results can be obtained for the Neumann (TE) modes (see⁶ for details).

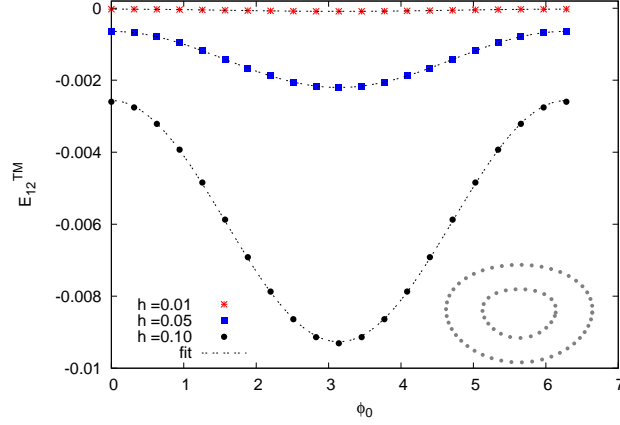


Fig. 2. Casimir interaction energy (TM modes) as a function of ϕ_0 for $\alpha = 2$ and different values of the perturbation h . The different shaped dots are the numerical data obtained with our program while the lines represent the numerical fit of each curve. Energies are measured in units of L/a^2 , and distances in units of a .

It is worth to remark that, when the amplitude of the corrugation is not very small, the exact results cannot be reproduced with a simple fit of the form $y(x) = A * \cos(x)$. This is illustrated in Fig.3, where we see that, for the biggest corrugated amplitude $\tilde{h} = h/a = 0.3$, the exact result differs from the cosine function.⁶

4. Outer conductors with focal lines: cylinder inside an ellipse

Some time ago, there was a conjecture⁹ based on a geometric optics approximation, about the possibility of focusing vacuum fluctuations in parabolic mirrors. It was argued that a parabolic mirror is capable of focusing the vacuum modes of the quantized electromagnetic field, therefore creating large physical effects near the mirror's focus. With this motivation, in this Section we shall evaluate the Casimir interaction energy for configurations

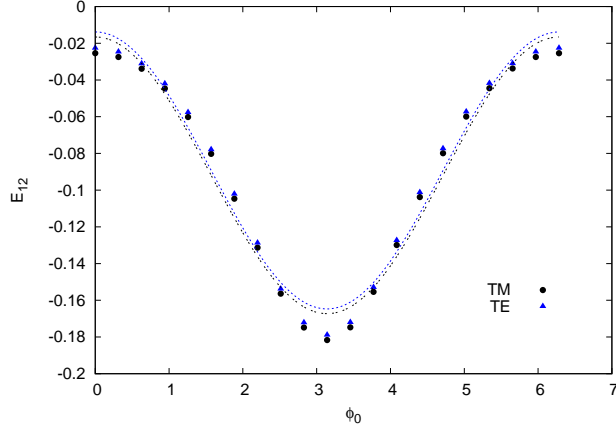


Fig. 3. Casimir interaction energy (TE and TM modes) as a function of ϕ_0 for $\alpha = 2$, $\nu = 3$ and $\hbar = 0.3$. The different shaped dots are the numerical data obtained by our program while the line represents the numerical fit of each curve. In this case, the plot shows that the exact result cannot be fitted by a function $y(x) = A * \cos(x)$. Energies are measured in units of L/a^2 .

in which the outer conducting shell has a cross section that contains focal points.

We will consider one small inner cylinder and an outer ellipse. We will denote by a the radius of the inner cylinder, by b_1 and b_2 the minor and major semi-axes of the ellipse, respectively, and by f the distance between the foci and the center of the ellipse. The coordinates of the center of the cylinder with respect to the center of the ellipse will be (ϵ_x, ϵ_y) . We will use an additional tilde to denote adimensional quantities, i.e. distances in units of a : $\tilde{b}_i = b_i/a$, $\tilde{f} = f/a$, etc.

For this configuration, we use a mesh where with an inner cylinder, and an outer ellipse with semi-axes $\tilde{b}_1 = 4$ and $\tilde{b}_2 = 4.33$. The ellipse has two focal points at $\tilde{f} = 1.66$. We present the results for the Casimir energy in Fig.4.

From Fig.4 it is possible to see that there is an unstable equilibrium position at the origin under displacements of the inner cylinder along the (vertical) ϵ_y direction. As expected, it is also possible to check that the energy grows as well as the cylinder gets closer to the surface of the outer ellipse. Fig.4 also shows a monotonic behaviour of the energy as a function of the position, even when passing through the focus. So we do not see a focusing of vacuum fluctuations near the focus of the ellipse. However, in

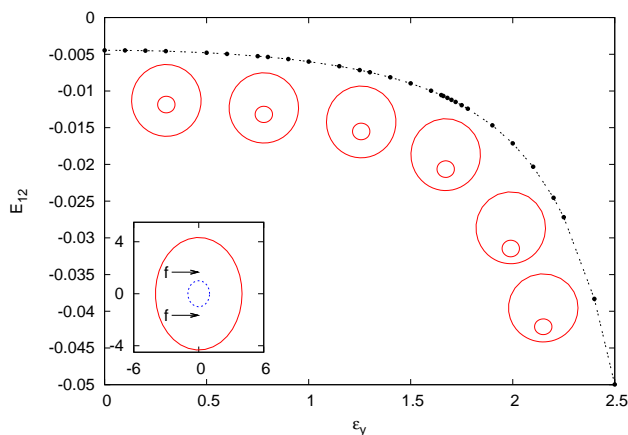


Fig. 4. Numerical evaluation of the Casimir interaction energy for an inner cylinder an eccentric outer ellipse, as a function of the position of the cylinder along the vertical axis. Energies are measured in units of L/a^2 .

order to confirm this result one should consider much smaller inner cylinders, in order to explore shorter wavelengths. This will require much more computational effort.

Finally, we have also checked⁶ that there is an unstable equilibrium position at the origin when moving the inner cylinder in the (horizontal) ϵ_x direction.

5. Final remarks

We have presented new numerical methods to compute the vacuum energy for arbitrary geometries with translational invariance. The approach is based on the use of traditional boundary methods to compute eigenvalues of the two dimensional Helmholtz equation, combined with Cauchy's theorem.

As a particular example, we have described a straightforward version of the point-matching method to compute the Casimir interaction energy for a waveguide with different permittivities, and reviewed some numerical calculations for perfect conductors. In all examples, for the numerical calculations we have chosen pair of points with the same angular coordinate with respect to the inner cylinder. For less symmetric configurations, and when the surfaces of both conductors are closer to each other, it will be necessary to consider grids with a larger number of points, and to optimize

their positions. As in the applications to acoustic or classical electromagnetism, special care must be taken for surfaces with pronounced edges, clefts or "handles", where the point-matching technique may not be accurate to determine the eigenfrequencies. In these cases, more sophisticated approaches⁴ could be necessary to optimize the numerical evaluation and to avoid spurious solutions.

We would like to thank Kim Milton for the organization and his kind hospitality during QFEXT09. This work has been supported by CONICET, UBA and ANPCyT, Argentina.

References

1. J.R. Kuttler and V.G. Sigillito, SIAM Review 26, 163 (1984).
2. R Bates, IEEE Trans. on Microwave Theory and Techniques, Vol. MTT-17, 297 (1969); H. Y. Yee and N.F.Audeh, IEEE Trans. on Microwave Theory and Techniques, Vol. MTT-13, 847 (1965); ibidem Vol. MTT-14, 487 (1966); J.R. Kuttler and V.G. Sigillito, SIAM Review 26, 163 (1984) and references therein. For a generalization and applications to scattering problems see F.M. Kahnert, J. Quant. Spectrosc. Radiat. Transfer **79-80**, 775 (2003) and references therein.
3. A. Karageorghis, Appl. Math. Lett. 14, 837 (2001); C.C. Tsai et al, Proc. R. Soc. A462, 1442 (2006).
4. J.V. Villadsen and E. Stewart, Chem. Engng. Sci. 22, 1483 (1967); T. Betcke and L.N. Trefethen, SIAM Review 47, 469 (2005) C.J.S. Alves and P.R.S. Antunes, CMC 2, 251 (2005); D. Cohen, N. Lepore and E.J. Heller, J. Phys. A: Math. Gen. 37, 2139 (2004); P. Amore, arXiv 0910.4798v1 [quant-ph].
5. A. Rodriguez, M. Ibanescu, D. Iannuzzi, F. Capasso, J. D. Joannopoulos, and S.G. Johnson, Phys. Rev. Lett. **99**, 080401 (2007).
6. F.C. Lombardo, F.D. Mazzitelli, P.I. Villar, and M. Vázquez, Phys. Rev. D**80**, 0605018 (2009).
7. F. D. Mazzitelli, F. C. Lombardo and P. I. Villar, J. Phys.: Conf. Ser. 161, 012015 (2009).
8. I. Cavero-Peláez, K.A. Milton, P. Parashar and K.V. Shajesh, Phys. Rev. D **78**, 065019 (2008).
9. L.H. Ford and N.F. Svaiter, Phys. Rev. A **62**, 062105 (2000).